Kovove Mater. 50 2012 251–257
DOI: 10.4149/km_2012_4_251

Change of solidification behaviors in the superheating Sn-40wt.%Bi alloy from the viewpoint of the relaxation of properties

G. H. Ding[1,2,3]*, X. F. Li[2], H. S. Chen[2]

[1] *School of Physics and Electronic Information, Huaibei Normal University, Huaibei 235000, China*
[2] *School of Materials Science and Engineering, Hefei University of Technology, Hefei 230009, China*
[3] *Anhui Key Laboratory of Energetic Materials, Huaibei 235000, China*

Received 19 September 2011, received in revised form 26 October 2011, accepted 11 November 2011

Abstract

The effects of melt overheating treatment on solidification of Sn-Bi alloys are studied from the viewpoint of the relaxation of properties. The results reveal that the change trends of cooling rate, undercooling degree of the primary and eutectic nucleation and maximum solidification rates of primary phase of melts not undergoing the relaxation are contrary to those of melts undergoing the relaxation. However, the change of these parameters could not explain the change on the microstructures. The present paper suggests the increasing of the apparent primary undercooling during solidification can be used to describe the refinement of primary phase after melts undergoing the relaxation. Our study may open new possibilities for the control of solidification process, which governs the microstructure, mechanical and physical properties of solids.

Key words: structural relaxation, alloys, crystal growth

1. Introduction

Melt superheating treatment has been widely explored and used in modifying the solidification microstructure and improving the physical properties of various materials: metallic alloys [1–3] and aerogels [4]. In developing semiconductors, melt overheating was shown to have a pronounced influence on defect formation (specifically, the melt overheat initiated the twins defect) during crystallization and improved the quality of ZnSe-based blue light-emitting laser diodes [5, 6]. By melt superheating, the morphology of the primary Mg_2Si particulates in the Mg_2Si/Al-Si-Cu composite changed from coarse dendritic to equiaxed, and their sizes decreased from larger than 150 μm to 40 μm [7]. Superheating treatment also affected the crystal growth kinetics and growth orientation of CdTe and PbTe alloys considerably [3].

However, selection of the optimum superheating temperature is still empirical or arbitrary, and adopting this method sometimes does not lead to the improvement of the microstructure [8]. Furthermore, although the effects of melt superheating on solidification have been somehow ascribed to different liquid structures, there was no convincing evidence for whether and how the structural change happened in the involved melts. On the other hand, the conventional view of liquids is that their structures and properties change gradually with temperature. Therefore, the exact mechanism of the melt superheating is still not fully understood, and there are discrepancies in the explanation put forward [9].

The conventional view considered the structure of a liquid varied smoothly from the melting to the critical point [10]. This view has been challenged over the past two decades by the observation of anomalies of various physical properties as a function of temperature at constant pressure [2, 11, 12]. More recently, both experimental findings and theoretical predictions have suggested the presence of liquid-liquid structural transitions (LLST) characterized by significant structural changes [13–16]. Furthermore, according to the

---

*Corresponding author: e-mail address: ghding@chnu.edu.cn

known melt structure information, the effect of the LLST on the solidified structures was investigated for some binary alloys, such as Al-Si [2], Pb-Sn [17], Bi-Sb [18] and Pb-Bi [19].

Sn-Bi alloys, as a kind of representative binary eutectic alloy and lead-free solder, have important research and application values [20–22]. In prior works, anomalous temperature dependence of internal friction [13], electrical resistivity [15], and viscosity [14] of liquid Sn-Bi alloys have suggested that the structural relaxation occurred. Further discussions on the mechanism of superheating treatment of liquid Sn-Bi alloys are not reported or elaborated in detail. Therefore, we expand on these aspects more explicitly in the current paper. There are three significant aspects of the work described in this paper: nucleation and growth mechanism and microstructural morphology.

2. Experimental

2.1. Solidification experimental procedure

The Sn-40wt.%Bi alloys are prepared from pure Bi (99.99 %) and Sn (99.99 %) granules, which were melted in Al_2O_3 crucibles and protected by B_2O_3 in the electrical resistance furnace. Each experiment used the equiponderant B_2O_3. The samples weighing 20 g were held in the corundum crucible at 600 ℃, 650 ℃, 700 ℃, 750 ℃, and 800 ℃ for 90 min, respectively. The sample at 600 ℃ was directly cooled to the room temperature in air. To observe the change of solidification behaviors in the same thermal condition, the others were quenched to 600 ℃ in a salt bath before cooled to the room temperature in air. The solidification microstructures were studied with the optical microscope after etching the samples.

In order to record the thermal history of the alloys during cooling, a type K thermocouple with quartz sheath was located at the same distance of 1 cm from the bottom of the mold symmetry axis to ensure reproducibility of the analysis. The temperature-time curves were recorded by the KEITHLEY-2182 nanovoltmeter. The cooling curves obtained were numerically processed using the Newton thermal analysis [23] in order to obtain information about the solidification kinetics of the region of the casting near to the thermocouple.

Figure 1 shows the typical microstructures commonly observed in the experimental probes. It can be seen that all samples show two main microconstituents, the primary phase, which correspond to the dendritic dark matrix and the eutectic microconstituent, present as the light. Here it can be observed that Fig. 1a,b differs greatly from Fig. 1c–e in the size and morphology of the primary phase. As the samples solidified in the same thermal condition, we ascribed the difference among the microstructures to the changes of liquid properties induced by superheating. For this purpose, the direct current four-probe technique was also used to study the evolution of the electrical resistivity of Sn-40wt.%Bi melt with time held at different overheating temperatures 600 ℃, 650 ℃, 688 ℃ and 742 ℃.

2.2. Electrical resistivity measurement

In many of our former investigations, the electrical resistivity method was used to study liquid alloys, which was proved to be valid and sensitive to liquid structural changes. For example, by comparing the results of Refs. [11, 24, 25], it is clear to see that the electrical resistivity behaviors of In-Sn liquid during heating process are in good accordance with those of internal friction and X-ray diffraction. Therefore, the direct current four-probe technique was also used in this paper to study the evolution of the electrical resistivity of Sn-40wt.%Bi melt with time during isothermal experiments.

The samples were prepared from 99.99 % pure bismuth and tin, which were melted at 400 ℃ for over 30 min, then poured into measuring cells for the following experiment. The measuring cells, manufactured from silica glass, 3.4 mm in diameter, were used in this experiment. Four tungsten electrodes, 1 mm in diameter, two for current and two for voltage, were placed in the end and central section wall of the cell, respectively. The space between the voltage electrodes was 2.8 cm. The voltage was measured with a high precision KEITHLEY-2182 nanovoltmeter, while a constant current of 500 mA was supplied by the PF66M sourcemeter. In the isothermal experiments, Sn-40wt.%Bi samples were heated rapidly to 600 ℃, 650 ℃, 688 ℃ and 742 ℃ at the rate of 200 K $\min^{-1}$, respectively, then held for the resistivity measurements. The resistivity measurements were carried out in purified argon media from which water had been removed by oil of vitriol to protect the sample from oxidation. In order to reduce the density segregation, the cell structure had a special horizontal design.

3. Results and discussion

The curves of resistivity versus time began to be recorded after the melts were heated to the preset temperatures, as shown in Fig. 2. From Fig. 2a, it can be observed clearly that the resistivity of the Sn--40wt.%Bi melt held at 600 ℃ for 330 min is almost unchanged. However, in Figs. 2b,c,d, there are all S-shaped changes in the curves after holding at each temperature for some time.

Since resistivity is one of the physical properties sensitive to structure, the result of Fig. 2a indicates

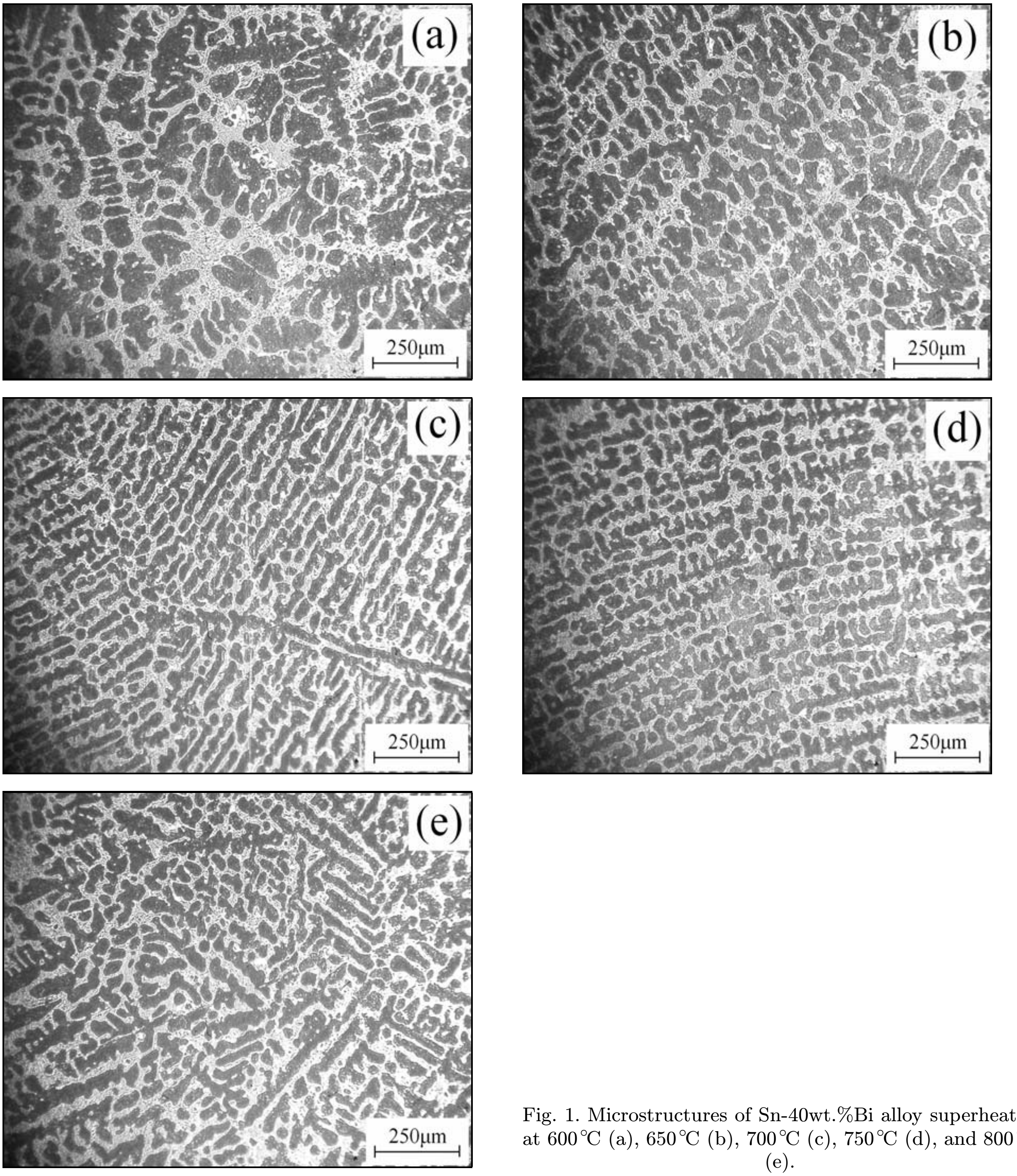

Fig. 1. Microstructures of Sn-40wt.%Bi alloy superheated at 600 °C (a), 650 °C (b), 700 °C (c), 750 °C (d), and 800 °C (e).

that the melt structural transition did not occur during the holding time and the influencing factors that might change the resistivity such as composition segregation can be neglected. Moreover, the effect of the density segregation on resistivity can be also ignored because the density difference between Bi and Sn will become smaller at the higher temperatures [10]. In Figs. 2b,c,d, the S-shapes reveal the resistivity relaxation in the Sn-40wt.%Bi melt held at 650 ℃, 688 ℃ and 742 ℃, which might be attributed to the melt structural transition although the absence of structure parameters, such as structure factor, atomic distance, etc. It is clear that the relaxation starting time, ending time and relaxation time become shorter at the higher temperature.

In this study, samples for solidification experiments were held at 600 ℃, 650 ℃, 700 ℃, 750 ℃ and 800 ℃ for 90 min, respectively. According to Fig. 2, the liquid properties of the samples at 600 ℃ and 650 ℃ do not relax, whereas they relax at 700 ℃, 750 ℃ and 800 ℃. When considered the heredity of liquid structures, the solidified microstructures and solidification

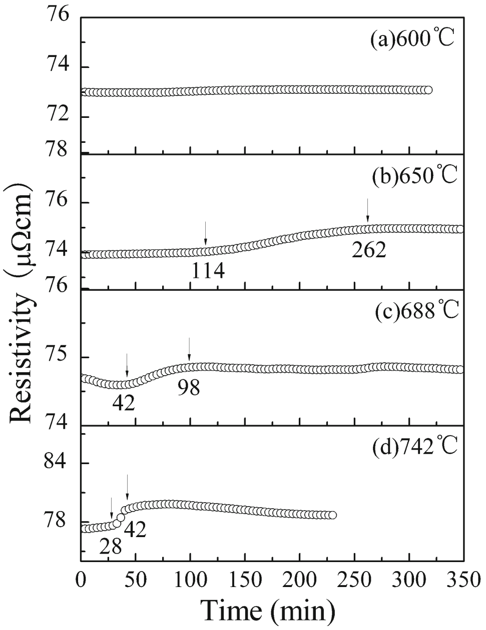

Fig. 2. Resistivity versus time for liquid Sn-40wt.%Bi alloy at different temperatures.

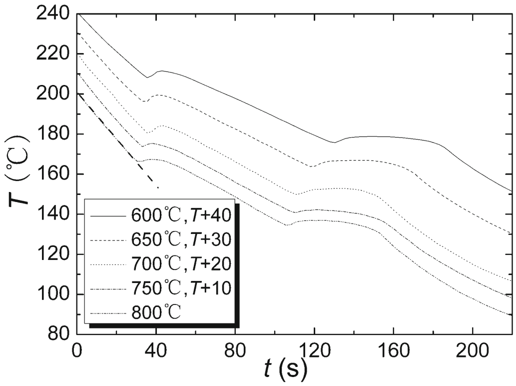

Fig. 3. Temperature-time curves of the Sn-40wt.%Bi alloys cooling from five different temperatures.

kinetics change with the relaxation of liquid properties or structures, which is just confirmed by Fig. 1.

Figure 3 shows cooling curves associated with the five superheating Sn-40wt.%Bi alloys. It can be readily seen that, as a result of the relaxation in liquid Sn-40wt.%Bi alloys, there is a decrease in the solidification time, which can be inferred from the shortening of the cooling curves corresponding to the alloys after the relaxation. In our research on the solidification of the Bi-Sb alloy [18], it can be observed that one of the effects of LLST is the decrease of the latent heat released during solidification. This effect in turn enhanced the cooling of the cast under more severe conditions, and caused the shortening of the solidification time. Here these phenomena during the solidification of superheating Sn-40wt.%Bi alloys could also be attributed to the decrease of the latent heat released during solidification as a result of the change in liquid structure, see Fig. 4.

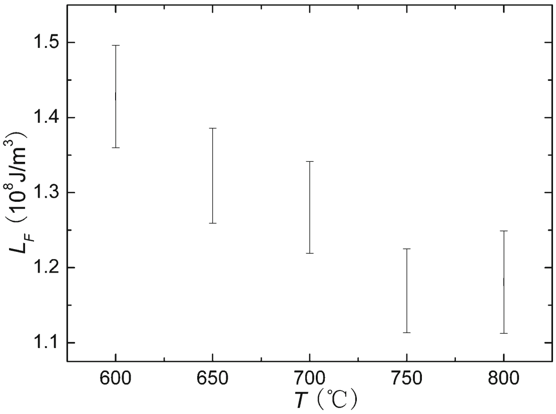

Fig. 4. Latent heat released during solidification for five superheating Sn-40wt.%Bi alloys.

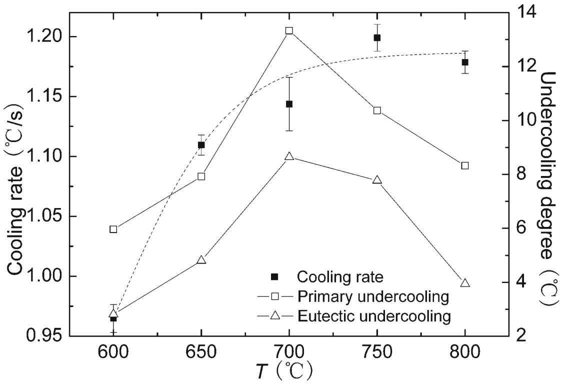

Fig. 5. Cooling rates, undercooling degree of the nucleation of primary and eutectic phase of the Sn-40wt.%Bi alloys superheating at different temperatures. The dash line is to guide the eye.

Moreover, Fig. 3 shows the different trend of the undercooling degree of the primary and eutectic nucleation before and after the relaxation, detailed in Fig. 5. The undercooling degrees of the primary and eutectic nucleation increase with the overheating temperature and get the maximum about 700 ℃, whereas the undercooling degrees of primary and eutectic phase decrease with temperature when the overheating temperature is above 700 ℃. In our solidification experiments, all samples were kept the same weight and cooled in air. Therefore, the difference of undercooling degrees could be attributed to the melt structure and the cooling rate.

In this paper, cooling rates were obtained from cooling curve data close to the liquidus temperature [26] (between 200 and 175 ℃), indicated by the dashed line in Fig. 3. Figure 5 shows the cooling rate after the relaxation is greater than that before the relaxation. Recently, Liu et al. [27] have mentioned that in Sn-Bi melts at low temperature above the liquidus temperature there are metastable clusters that are broken with temperature rising until the melt reaches a stable state with a new liquid structure. Prior investigations have indicated that some physical parameters including thermal conductivity [28], heat capacity [16, 28–30] and density [28, 31] are sensitive to liquid structure. It can be expected that, if the liquid structure changes its thermal diffusivity, which includes heat capacity and density, they may change. Before solidification a lumped heat balance can be written as:

$$-qA = mC_\mathrm{p}\frac{\mathrm{d}T}{\mathrm{d}t}, \tag{1}$$

where q ($\mathrm{J\,m^{-2}\,s^{-1}}$) is the heat flux leaving the system through the exchange area A ($\mathrm{m^2}$), m (kg) is the mass of the sample, C_p ($\mathrm{J\,kg^{-1}\,K^{-1}}$) is the heat capacity of the sample. And the cooling rate can be obtained from:

$$\frac{\mathrm{d}T}{\mathrm{d}t} = -\frac{qA}{mC_\mathrm{p}}. \tag{2}$$

If the mass m and the heat extraction conditions ($-qA$) are the same for all the samples, the change in $\mathrm{d}T/\mathrm{d}t$ implies a change in the C_p of the samples. DTA measurements of prior investigations [16, 28–30] showed the melts absorbed heat during LLST. This result implied that C_p may decrease with LLST. According to Eq. (2), the cooling rate after the relaxation is greater than that before the relaxation.

Commonly, with faster cooling rates, the degrees of undercooling should be expected to increase. Hence, the decrease of undercooling degree of the melts above 700 ℃ could be considered to be induced by the relaxation. During the nucleation of the main microconstituents, when maximum undercooling increases, this indicates less availability of substrates that could be used as heterogeneous nuclei. Moreover, if maximum undercooling decreases, that means that there are more substrates available for heterogeneous nucleation. Perhaps the substrates which operate with the liquid with "normal structure" at low temperature, dissolve with increasing temperature up to the critical temperature and as the liquid structure changes, new substrates are triggered, which grow more slowly because of the presence of a higher energy barrier. What is clear is that the nucleation behavior of both microconstituents changes as a result of the change in the structure of the liquid.

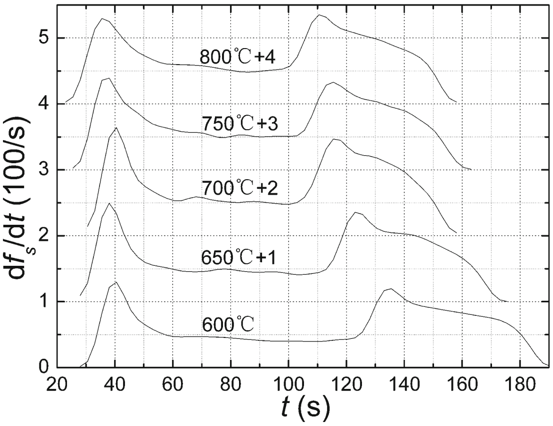

Fig. 6. Solidification rates of Sn-40wt.%Bi alloys superheating at different superheating temperatures.

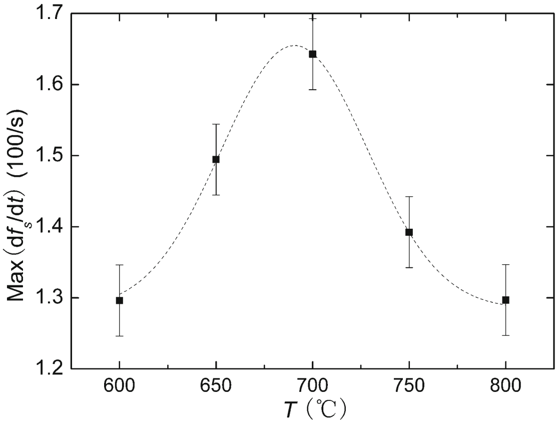

Fig. 7. Maximum values of solidification rates of primary phase vary with superheating temperature.

During solidification, the nucleation rate is sensitive to temperature changes [32]. Change of undercooling degree as a result of the relaxation gives place to the changes of nucleation in the solidification. Figure 6 shows the solidification rate evolution that results from the numerical analysis of the experimental cooling curves for the cases studied in this work, following the Newton thermal analysis procedure [23]. The local solidification rates shown in this figure are related to the solidification events that occurred in the central region of the castings. For the hypoeutectic Sn-40wt.%Bi alloy, two maxima can be observed on the solidification rate curves. The first maximum corresponds to the solidification of the primary phase and the second is related to the eutectic solidification.

According to the viewpoint of Kurz and Fisher [32], the first maximum value is nucleation-controlled. Figure 7 shows that the first maximum values increase with temperature when the melts are overheated below 700 ℃, on the contrary, above 700 ℃, the maximum values decrease with temperature. Decreasing undercooling of primary phase solidification could explain the observed decrease in the maximum solidi-

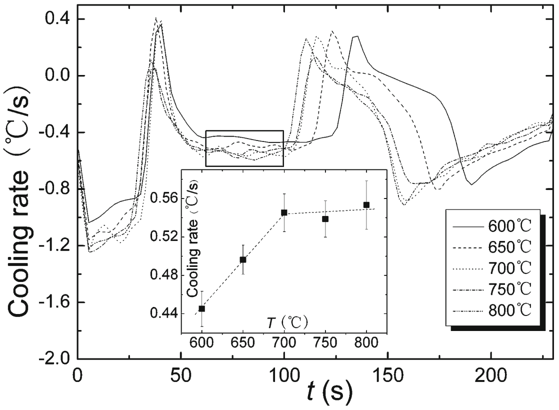

Fig. 8. Cooling rates as a function of time for superheating Sn-40wt.%Bi alloys. The cooling rates during the growth are the averages of values in the pane for different superheating temperature, and the calculated rates are shown in the inset.

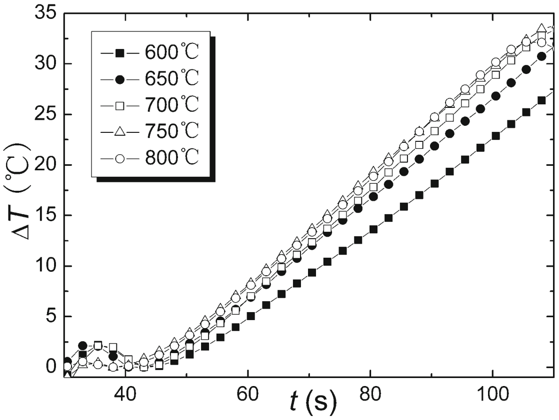

Fig. 9. Apparent primary undercooling as a function of time for superheating Sn-40wt.%Bi alloys.

fication rate when melts are undergoing the relaxation. This phenomenon indicates that the relaxation has a great nucleation-controlled effect on the dendritic primary phase.

In Fig. 1, the secondary dendrite arm spacing before the relaxation is coarser than those after the relaxation, and above all, the secondary dendrite arms after the relaxation are far longer than those before the relaxation and the tertiary dendrite arms appear in the samples held at 750 ℃ and 800 ℃. Kurz and Fisher [32] considered that the solidification was controlled by growth besides by nucleation. Commonly, with greater undercooling degree, the solidified microstructure should be refined [32, 33]. When the superheating temperature is below 700 ℃, the secondary dendrite arms are refined with undercooling degree increasing. However, above 700 ℃, the secondary dendrite arms are not re-coarsened with undercooling degree decreasing.

In order to explain the presence of the refined secondary dendrite arms at the thermal center of the Sn-40wt.%Bi alloys undergoing the relaxation, Fig. 8 shows the cooling rate evolution. Here, it can be observed that the secondary dendrite arms solidify under the greater cooling rate promoting greater apparent primary undercooling, when the melts undergo the relaxation. Figure 9 shows the apparent primary undercooling as a function of time. The concept of apparent primary undercooling comes of that of the apparent eutectic undercooling [34], and the primary undercooling is calculated taking into account the maximum recalescence temperature instead of the liquidus temperature. The eutectic growth theories [33, 35] indicate that an increase in the operating undercooling during solidification promotes a finer eutectic microstructure, with narrow spacings between eutectic lamellae. It can be seen on Fig. 9 that during solidification the apparent primary undercooling degrees after the relaxation are greater than those before the relaxation. Hence, NTA results indicate that liquid metal after the relaxation solidifies under the greater degree of undercooling, and this in turn implies the presence of fine primary phase as shown by metallographic findings (Fig. 1).

4. Conclusions

1. The cooling rate after the relaxation is greater than that before the relaxation. However, the undercooling degrees of the primary and eutectic nucleation increase with the overheating temperature and get the maximum about 700 ℃, whereas the undercooling degrees of primary and eutectic phase decrease with temperature when the overheating temperature is above 700 ℃. The different trends of undercooling degree could be considered to be induced by the relaxation.

2. The relaxation has greatly the nucleation-controlled effect on the dendritic primary phase. The maximum solidification rates of primary phase increase with temperature when the melts are overheated below 700 ℃, on the contrary, above 700 ℃, the maximum rates decrease with temperature.

3. The solidified microstructures of the superheating Sn-40wt.%Bi alloy are greatly different in the size and morphology of the primary phase. The secondary dendrite arm spacing before the relaxation is coarser than that after the relaxation, and above all, the secondary dendrite arms after the relaxation are far longer than those before the relaxation and the tertiary dendrite arms appear in the samples held at 750 ℃ and 800 ℃. The relaxation enlarges the apparent primary undercooling degrees during solidification. The increasing of the apparent primary undercooling

degree can explain the presence of fine primary phase as shown by metallographic findings.

Acknowledgements

The authors are very grateful to the National Natural Science Foundation of China (Grant No. 51101067), Anhui Key Laboratory of Energetic Materials (Grant No. KLEM2009003) and Anhui University Provincial Natural Science Research Project (Grant No. KJ2010B188) for financial supports.

References

[1] Wang, W. M., Bian, X. F., Qin, J. Y., Syliusarenko, S. I.: Metall. Mater. Trans. A, *31*, 2000, p. 2136.

[2] Bian, X. F., Wang, W. M.: Mater. Lett., *44*, 2000, p. 54. doi:10.1016/S0167-577X(00)00011-2

[3] Rudolph, P., Koh, H. J., Schaeffer, N., Fukuda, T.: J. Cryst. Growth, *166*, 1996, p. 578. doi:10.1016/0022-0248(96)00119-4

[4] Vollet, D. R., Donatti, D. A., Ruiz, A. I., d. Castro, W. C.: J. Non-Cryst. Solids, *332*, 2003, p. 73. doi:10.1016/j.jnoncrysol.2003.09.003

[5] Rudolph, P., Schaeffer, N., Fukuda, T.: Mater. Sci. Eng. R, *15*, 1995, p. 85. doi:10.1016/0927-796X(95)00182-4

[6] Wang, J. F., Omino, A., Isshiki, M.: Mater. Sci. Eng. B, *83*, 2001, p. 185. doi:10.1016/S0921-5107(01)00512-8

[7] Qin, Q. D., Zhao, Y. G., Liang, Y. H., Zhou, W.: J. Alloy. Compd., *399*, 2005, p. 106. doi:10.1016/j.jallcom.2005.03.015

[8] Bolotov, Y. A.: Refract. Ind. Ceram., *36*, 1995, p. 92.

[9] Qiu, D., Zhang, M. X., Taylor, J. A., Fu, H. M., Kelly, P. M.: Acta Mater., *55*, 2007, p. 1863. doi:10.1016/j.actamat.2006.10.047

[10] Iida, T., Guthrie, R. I. L.: The Physical Properties of Liquid Metals. Oxford, Clarendon Press 1993.

[11] Zu, F. Q., Zhu, Z. G., Guo, L. J., Qin, X. B., Yang, H., Shan, W. J.: Phys. Rev. Lett., *89*, 2002, p. 125505. doi:10.1103/PhysRevLett.89.125505

[12] Bellissent, R., Descotes, L., Boue, F., Pfeuty, P.: Phys. Rev. B, *41*, 1990, p. 2135. doi:10.1103/PhysRevB.41.2135

[13] Wu, A. Q., Guo, L. J., Liu, C. S., Jia, E. G., Zhu, Z. G.: Physica B, *369*, 2005, p. 51. doi:10.1016/j.physb.2005.08.003

[14] Wang, L., Bian, X. F., Liu, J. T.: Phys. Lett. A, *326*, 2004, p. 429. doi:10.1016/j.physleta.2004.04.052

[15] Li, X. F., Zu, F. Q., Ding, H. F., Yu, J., Liu, L. J., Xi, Y.: Phys. Lett. A, *354*, 2006, p. 325. doi:10.1016/j.physleta.2006.01.058

[16] Greenberg, Y., Yahel, E., Caspi, E. N., Benmore, C., Beuneu, B., Dariel, M. P., Makov, G.: Europhys. Lett., *86*, 2009, p. 36004. doi:10.1209/0295-5075/86/36004

[17] Xi, Y., Zu, F. Q., Liu, L. J., Shen, R. R., Li, X. F., Chen, Z. H.: Kovove Mater., *43*, 2005, p. 432.

[18] Zu, F. Q., Ding, G. H., Li, X. F.: J. Cryst. Growth, *310*, 2008, p. 397. doi:10.1016/j.jcrysgro.2007.10.031

[19] Zu, F. Q., Chen, J., Li, X. F., Mao, L. N., Liu, Y. C.: J. Mater. Res., *24*, 2009, p. 2378. doi:10.1557/jmr.2009.0294

[20] Asryan, N. A., Mikula, A.: Inorg. Mater., *40*, 2004, p. 386. doi:10.1023/B:INMA.0000023961.34926.67

[21] Yasuda, H., Ohnaka, I., Kawasaki, K., Sugiyama, A., Ohimichi, T., Iwane, J., Umetani, K.: J. Cryst. Growth, *262*, 2004, p. 645. doi:10.1016/j.jcrysgro.2003.09.052

[22] Castro, W. B. D., Kiminami, C. S.: J. Mater. Sci. Lett., *18*, 1999, p. 487. doi:10.1023/A:1006602716724

[23] Barlow, V. O., Stefanescu, D. M.: AFS Trans., *105*, 1997, p. 349.

[24] Shen, R. R., Zu, F. Q., Li, Q., Xi, Y., Li, X. F., Ding, G. H., Liu, H. M.: Phys. Scr., *73*, 2006, p. 184. doi:10.1088/0031-8949/73/2/010

[25] Zu, F. Q., Li, X. F., Guo, L. J., Yang, H., Qin, X. B., Zhu, Z. G.: Phys. Lett. A, *324*, 2004, p. 472. doi:10.1016/j.physleta.2004.03.014

[26] Venkaltaramani, R., Simpson, R., Ravindran, C.: Mater. Charact., *35*, 1995, p. 81. doi:10.1016/1044-5803(95)80096-4

[27] Liu, L. J., Liu, M. Q., Zu, F. Q., Huang, Z. Y., Hu, C. M., Mao, L. N.: Phys. Chem. Liq., *48*, 2010, p. 329. doi:10.1080/00319100902839152

[28] Sobolev, V.: J. Nucl. Mater., *362*, 2007, p. 235. doi:10.1016/j.jnucmat.2007.01.144

[29] Zu, F. Q., Zhu, Z. G., Guo, L. J., Zhang, B., Shui, J. P., Liu, C. S.: Phys. Rev. B, *64*, 2001, p. 180203. doi:10.1103/PhysRevB.64.180203

[30] Chen, Z. H., Zu, F. Q., Li, X. F., Yu, J., Xi, Y., Shen, R. R.: J. Phys. Condens. Matter, *19*, 2007, p. 116106. doi:10.1088/0953-8984/19/11/116106

[31] Geng, H. R., Zhang, G. L., Wang, Z. M., Deng, Y. B., Qin, H. O.: Appl. Phys. A, *98*, 2009, p. 227. doi:10.1007/s00339-009-5380-2

[32] Kurz, W., Fisher, D. J.: Fundamentals of Solidification. Uetikon-Zuerich, Trans Tech Publications 1998.

[33] Trivedi, R., Kurz, W.: Acta Metall. Mater., *42*, 1994, p. 15. doi:10.1016/0956-7151(94)90044-2

[34] Gonzales-Rivera, C., Campillo, B., Castro, M., Herrera, M., Juarez-Islas, J.: Mater. Sci. Eng. A, *279*, 2000, p. 149.

[35] Magnin, P., Trivedi, R.: Acta Metall. Mater., *39*, 1991, p. 453. doi:10.1016/0956-7151(91)90114-G